

Lusi Ernawati<sup>1</sup>, Ruri Agung Wahyuono<sup>2</sup>, Abdul Halim<sup>3</sup>, Nurul Widiastuti<sup>4</sup>, Audi Sabrina<sup>1</sup> & Kurnia Handayani<sup>1</sup>

<sup>1</sup>Department of Chemical Engineering, Institut Teknologi Kalimantan, Jalan Soekarno Hatta, KM 15, Karang Joang, North Balikpapan, 76127, East Kalimantan, Indonesia
 <sup>2</sup>Department of Engineering Physics, Institut Teknologi Sepuluh Nopember, Jalan Arief Rahman Hakim, Keputih, Sukolilo, Surabaya, 60111, East Java, Indonesia
 <sup>3</sup>Department of Chemical Engineering, Universitas Internasional Semen Indonesia, Jalan Veteran, Kb. Dalem, Sidomoro, Kebomas, Gresik, 61122, East Java, Indonesia
 <sup>4</sup>Department of Chemistry, Institut Teknologi Sepuluh Nopember, Jalan Arief Rahman Hakim, Keputih, Sukolilo, Surabaya, 60111, East Java, Indonesia

\*E-mail: r agung w@ep.its.ac.id

#### **Highlights:**

- Silk fibroin/soursop seeds (SF/SS) powder shows superior dye and heavy metal adsorption capability up to 87.3% and 93.7%, respectively.
- The kinetics of heavy metal ions (Cu<sup>2+</sup>) and crystal violet adsorption followed the Langmuir and Freundlich models.
- This is the first investigation into a bio-adsorbent made from a silk fibroin/soursopseed (SF/SS) composite.

Abstract. Groundwater highly contaminated with organic substances and heavy metal ions in the Kariangau Industrial Area, Balikpapan, East Kalimantan is indicated by the comparatively high COD. Therefore, the technology for treating wastewater to remove various toxins before releasing it into the environment needs to be advanced. Here, we present a green synthetic method of a composite adsorbent (SF/SS) using soursop seeds and silkworm cocoons. SEM, FTIR, and BET were used to analyze the physicochemical characteristics of the adsorbent. Mechanistic investigation of the SF/SS adsorbent performance for the removal of Cu<sup>2+</sup> metal ions and crystal violet (CV) was conducted, while taking into account variables affecting adsorption properties. The Freundlich and Langmuir isotherm adsorption models were used to fit the adsorption equilibrium, while pseudo-first and second-order models were used to assess the adsorption kinetics. The mesoporous SF/SS adsorbent exhibited the highest adsorption capacities of 78.6 and 69.2 mg·g<sup>-1</sup>, respectively. The pseudo-first model showed the best fit for CV removal with a kinetic rate of 0.0634 min<sup>-1</sup>, while the Freundlich model exhibited the best fitting for both of CV and Cu<sup>2+</sup> removal. The results showed that SF/SS can be applied as an efficient adsorbent for both of heavy metal and organic dye removal.

**Keywords:** adsorption; dye molecules; heavy metals; organic pollutants; silkworm cocoons; water remediation.

#### 1 Introduction

Kariangau Industrial Zone (KIZ) in Balikpapan, East Kalimantan, is classified as an integrated industrial zone for large and medium-sized businesses as well as warehousing operations. This zone accommodates a variety of industries, including coal, oil and gas, commodities, aquaculture, and other business sectors [1]. The handling of significant quantities of pollutants, including organic dyes and solvents, hydrocarbons, heavy metals, and other hazardous compounds is the result of this circumstance. These pollutants also have a significant chance of having an adverse direct or indirect impact on the groundwater. According to the literature, the groundwater and coastal garbage around KIZ are contaminated by organic matter and have a high concentration of heavy metal ions, including Pb (28.43 ppm), Cd (28.67 ppm), Cu (26.49 ppm), and As (19.08 ppm) [2-3]. Numerous health problems, including poor drinking water quality, the loss of water supply, deteriorated surface water systems, and high costs for alternative water sources, could be brought on by this contaminated groundwater [4].

Up until recently, activated carbon has been commonly used as adsorbent for these pollutants [5,6]. However, the high cost and difficult regeneration and separation processes of activated carbons limit their usefulness in water treatment [7]. A variety of renewable materials, such as rice husk, sugar beet pulp, soybean, hulls, clay, and tea waste, have developed as alternative, abundant adsorbents for heavy metals and organic compound removal [8,9]. Due to their accessibility, eco-friendliness, and affordability, these materials have attracted a lot of interest. However, some of them show a poor capacity and a slow rate of adsorption [9,10]. Therefore, there is still a need for research into highly effective bio adsorbents for environmental remediation. One of the numerous biopolymers that has attracted a lot of interest is silk fibroin (SF), which is non-toxic, biodegradable, and has great biocompatibility [12,13]. Consequently, SF is also intensively utilized in foods, cosmetics, textiles, and clothing [14,15].

Bio-composite foams formed from powdered orange peel and SF have been reported as an adsorbent for methylene blue [16,17]. Despite its limited adsorption capacity, orange peel waste has the potential to increase its value as a potential water treatment material by being included in a highly porous bio-composite foam. According to other studies, SF can also take up metal ions by binding them to the amide group of oxygen or nitrogen atoms in its amino acid composition [18,19]. Additionally, the hydrophilic and amphoteric characteristics of SF allow it to interact with a variety of dye molecules. The aforementioned factors suggest that wastewater treatment employing SF-based bio-adsorbent may be developed.

Here, we present an SF-based bio-composite adsorbent for removing Cu<sup>2+</sup> and crystal violet (CV) dye in conjunction with soursop seeds (SS). We outline a green method for creating an adsorbent made of silk fibroin (SF), which is obtained from silkworm cocoons, and then we describe how to create an SF/SS bio-composite via wet-chemical synthesis. The adsorption parameters, including the adsorbent compositions, and initial pollutant concentrations, affecting the performance of SF/SS adsorption were carefully investigated.

The adsorption isotherms and kinetics of Cu<sup>2+</sup> and CV dyes are described. Additionally, this work presents the first development of a bio-composite adsorbent for the removal of heavy metal ions and dye pollutants from wastewater, which is made of SS particles controlling the pore structure of a solid matrix based on SF. This work also shows that even without freeze drying process, which takes a higher amount of energy for synthesis, the current SF/SS composites somehow exhibit a controllable architecture of adsorbent morphology similar to our earlier findings [19]. Further study into bio-composite adsorbents may also be possible as a result of the exploration of these SF/SS-based compounds.

#### 2 Experiment

#### 2.1 Materials

The *Bombyx mori*-silkworm cocoons, copper (II) sulfate pentahydrate (CuSO<sub>4</sub>.5H<sub>2</sub>O, MERCK) and crystal violet were bought from chemical provider (NG company) and kept in a desiccator overnight. Local soursop seeds were cleaned using water and further using 0.2 M HCl (Sigma-Aldrich) for 24 hours. Other chemical agents, i.e., sodium carbonate anhydrous (Na<sub>2</sub>CO<sub>3</sub>, MERCK), calcium chloride dihydrate (CaCl<sub>2</sub>.2H<sub>2</sub>O, MERCK), distilled water, and ethanol, were utilized exactly as received.

## 2.2 Extraction of Silk Fibroin (SF)

We sliced up the silkworm cocoons and extensively cleaned them in a boiled 0.5% Na<sub>2</sub>CO<sub>3</sub> distilled water solution for 30 minutes. The sample was then washed for 30 minutes with the same solution at 40 to 50 °C. After drying and left overnight in a desiccator, the obtained sample of pure silk fibroin (SF) was transformed into degummed silk. The degummed SF 1/20 (w/v) was dissolved in a mixed solvent (CaCl<sub>2</sub>/H<sub>2</sub>O/EtOH of 111/144/92 in weight), and then agitated at 80 °C for 2 hours. The resulting SF was then dialyzed in deionized water for 48 hours. To prevent the SF volume from rising, the dialysis was performed in a dialyses cassette (MW Cut-off: 12.000-14.000) with a 1-L capacity. The solvent

was switched out every 30 minutes for the first two hours, then every 12 hours for the next two days.

### 2.3 SF/SS Bio-Composite Adsorbent

In order to prepare SF/SS bio-adsorbent composites, soursop seed (SS) dried powder with certain compositions was added to the SF solution in two different amounts: 1 g of SF/SS (4:1) and 2 g of SF/SS (3:2). The mixed solution was ultrasonically treated for 30 minutes, until it gelled. The final gel was then baked for two hours at 90 °C before being placed in a freezer for the night.

# 2.4 Adsorption Analysis for Crystal Violet and Cu<sup>2+</sup> Removal

The removal of crystal violet (CV) and Cu<sup>2+</sup> ions from CuSO<sub>4</sub>.5H<sub>2</sub>O in wastewater was examined using SF/SS composite as an adsorbent. In 50-mL glass bottles, batch adsorption tests were conducted using a specific volume of dried SF/SS. Adsorption tests were performed in a series of batch systems as a function of the initial dye concentration (10, 20, and 50 ppm), contact time, and adsorbent dosage (150 mg). Centrifugation and filtration were used to separate out a portion of the solution at predefined intervals of time. All collected solutions were removed from the adsorbent after each batch of adsorption tests, and a spectrophotometer was used to determine the dye concentration at maximum absorbance (700 nm). The experiments had a standard deviation of 6.0% and were performed in triplicate. The calculated adsorption capacity was analyzed using the *Langmuir* and *Freundlich* isotherms, and the adsorption kinetics were calculated using pseudo-first order (PFO) and pseudo-second order (PSO) models.

#### 2.5 Materials Characterization

The morphology of SF/SS composites was examined using scanning electron microscopy (SEM, HITACHI-SU-3500) with an accelerating voltage of 10 kV. The IR spectra of the resulting SF and SF/SS composites were analyzed using a Spectrum BX (PerkinElmer) spectrometer in the spectral region of 400 to 4000 cm<sup>-1</sup>. Using a BET (NOVA 4200E) device, the N<sub>2</sub> adsorption and desorption isotherms were determined at 77 K with the heating rate of 5 °C/min. Before the BET test, the material was dried for three hours at 200 °C in N<sub>2</sub>.

#### 3 Results and Discussions

# 3.1 Physicochemical Properties of SF and SF/SS Biocomposite Adsorbent

Figure 1 depicts the morphology of the bio-composite adsorbent made of SF and SF/SS. Irregular forms were visible on the dried SF powder surface, as shown in Figure 1(a). The contraction of the SF during drying may be related to this. The SF/SS (3:2) and SF/SS (4:1), however, both have porous surfaces with some noticeable fissures. This pore structure is crucial in facilitating diffusion and increasing the specific surface area, which can favor the adsorption of adsorbate molecules, i.e., CV and Cu<sup>2+</sup> [20]. When SF and SF/SS surfaces are compared, it is evident that SF/SS has interconnected pores, whereas pure SF essentially has no pores at all. This lack of pores is probably caused by the high hydrophilicity of SF.

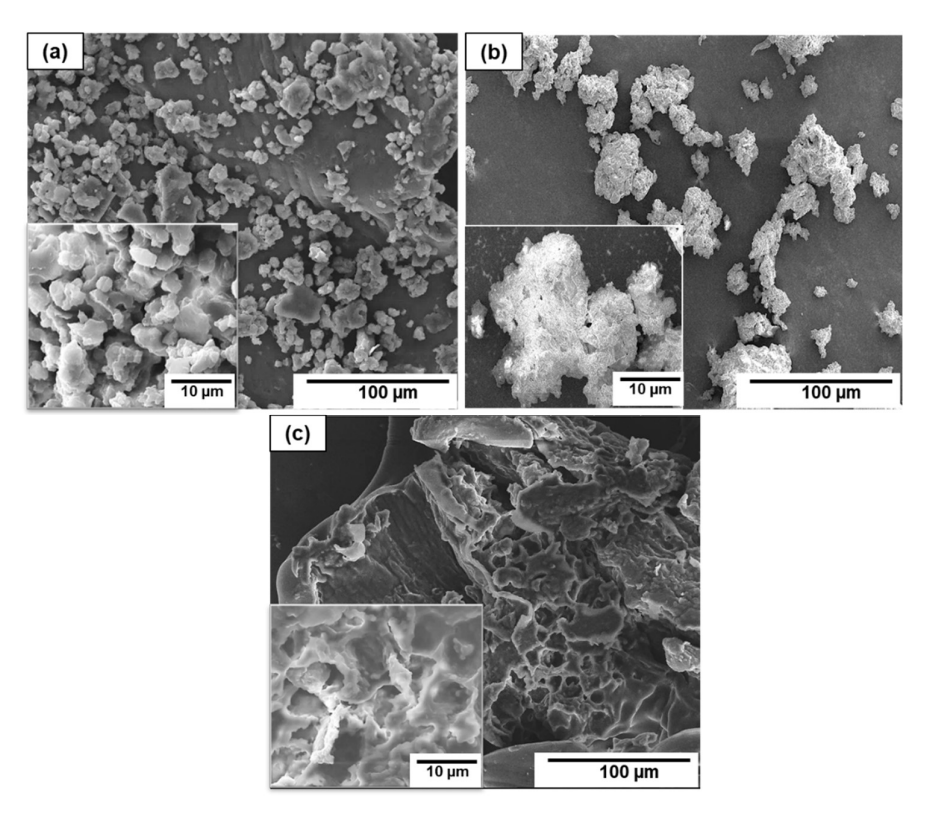


Figure 1 SEM micrograph of (a) pure SF, (b) SF/SS (3:2), and (c) SF/SS (4:1).

Irrespective of the composition, the pore opening in SF/SS due to compositing with soursop seeds indicates that the soursop seeds contain a cross-linking agent, presumably phytic acids [19], that affects the pore structure of bio-composites. An amount of 20% SS in SF/SS (4:1) creates a lamellar structure of interconnected SF with a large porous structure, while 40% SS in SF/SS (3:2) breaks the agglomeration of SF/SS bio-composite and decreases the pore size on the surface. This reflects that the soursop composition can indeed control the pore structure of bio-composite adsorbent and, hence, optimization of SF/SS composition is suggested.

In the above discussion, the morphology and pore structure, which will be detailed later in the BET characterization, are important parameters to control since they provide adsorption sites for organic molecules as well as heavy metal ions. However, it should be noted that functionalization of the SF/SS adsorbent surface is also important, since it determines the adsorption mechanism and the strength with which the organic molecules and cations bind to the surface. In this study, the electronic nature of pristine SF as indicated from the IR spectra is shown in Figure 2(a).

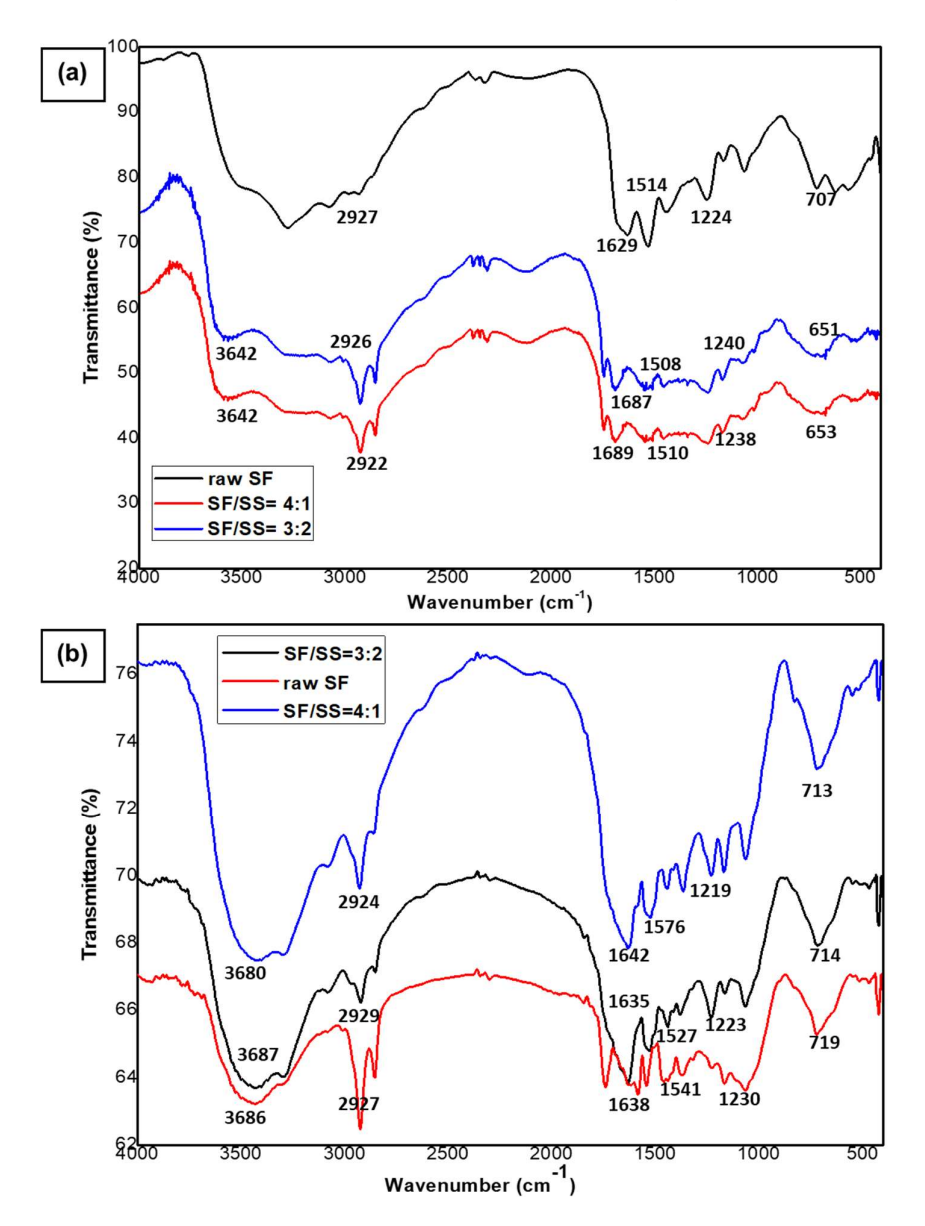
The spectral response exhibited absorption peaks at 3423 cm<sup>-1</sup> and 3174 cm<sup>-1</sup>, which are attributed to the -NH stretching of the secondary amide. C-H stretching is characterized by absorption peaks at 2927, 2926, 2922 cm<sup>-1</sup>, while peaks at 1643 cm<sup>-1</sup>, 1545 cm<sup>-1</sup>, and 1687, 1689, 1629 cm<sup>-1</sup> can be assigned to C=O stretching, -NH bending, and amide-I (C=O stretching,  $\beta$ -sheet,  $\beta$ -turn), respectively [21]. The amide-II (NH-deformation), which is a lineament for the  $\beta$ -sheet of silk [22], is indicated by the adsorption band at 1508, 1510, and 1514 cm<sup>-1</sup> for both pure SF and pure SF/SS composite.

The absorption band emerges at 1224, 1238, and 1240 cm<sup>-1</sup> for the functional group of amide-III (CN stretching and NH bending,  $\beta$ -sheet), whereas the amide-IV is responsible for the absorption band at 651, 653, and 707 cm<sup>-1</sup>. At 3642 cm<sup>-1</sup> [23], the OH absorption of pure SF and SF/SS composite can be seen, with the latter exhibiting significantly larger absorption than that of pristine SF.

The IR spectra of the SF and SF/SS composite after CV adsorption tests are depicted in Figure 2(b), and the corresponding peak assignment is summarized in Table 1. The raw SF exhibited IR bands at 1638 cm<sup>-1</sup> (amide I) and 1547 cm<sup>-1</sup> (amide II), showing the primary structure of the β-sheet for SF. For both SF/SS compositions, the peak of the amide I group may be found at 1635-1642 cm<sup>-1</sup>.

The hydroxyl and amino groups of SF are responsible for the broad absorption peak, which is located at 3680, 3687, and 3686 cm<sup>-1</sup> [24]. Particularly notable is the peak shift of the amide II, amide III, and amide IV absorption bands. This

amide peak shift is due to an interaction between the carboxyl group of SF and the active site of CV that results in a new amide bond being formed.



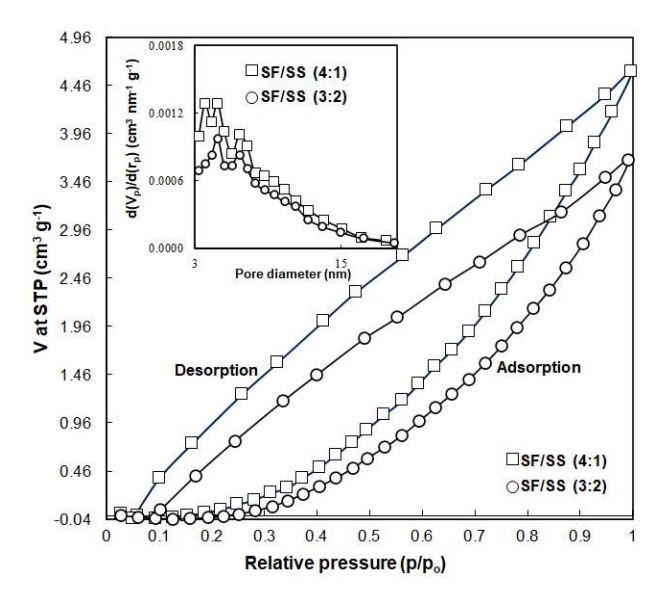
**Figure 2** Infrared spectra of silk fibroin and SF/SS composites: (a) dried SF powder before CV adsorption; and (b) after CV adsorption.

Table 1 Peak identifications in SF/SS FTIR spectra before and after CV adsorption.

Dried SF/SS powder	Peaks (cm <sup>-1</sup> )	Peak Assignments	
	1687, 1689, 1629 cm <sup>-1</sup>	Symmetric stretching of amide I (C=O, β-sheet, β-turn)	
	3423, 3174 cm <sup>-1</sup>	Bending of β-sheet, NH group	
	1545 cm <sup>-1</sup>	Stretching of amide II (C=O, β-sheet)	
Dofous CV	2927, 2926, 2922 cm <sup>-1</sup>	Asymmetric bending C-H group	
Before CV adsorption	1508, 1510, 1514 cm <sup>-1</sup>	Stretching of amide II (NH deformation, β-sheet conformation)	
	1224, 1238, 1240 cm <sup>-1</sup>	Stretching and bending of amide III (CN stretch and NH bends)	
	651, 653, 707 cm <sup>-1</sup>	Stretching of amide IV	
	3642 cm <sup>-1</sup>	Stretching of OH group	
	1642, 1635, 1638 cm <sup>-1</sup>	Symmetric stretching of amide I (C=O, β-sheet, β-turn)	
	3431, 3172 cm <sup>-1</sup>	Bending of β-sheet, NH group	
	1547 cm <sup>-1</sup>	Stretching of amide II (C=O, β-sheet)	
After CV adsorption	2924, 2929, 2927 cm <sup>-1</sup>	Asymmetric bending of C-H group	
	1527, 1541, 1576 cm <sup>-1</sup>	Stretching of amide II (NH deformation)	
	1219, 1223, 1230 cm <sup>-1</sup>	Stretching and bending of amide III (CN stretches and NH bends)	
	651, 653, 707 cm <sup>-1</sup>	Stretching of amide IV	
	3680, 3687, 3686 cm <sup>-1</sup>	Stretching of OH group	

The detailed surface features were evaluated using BET characterization and BJH (Barrett, Joyner, and Halenda) analysis since the adsorption of organic dyes and heavy metals largely depends on the surface properties of the adsorbent. The physical characteristics of the SF/SS biocomposite resulting from the N<sub>2</sub> adsorption-desorption isotherm are shown in Figure 3. The BET formula was utilized to estimate the specific surface area of SF/SS, while the BJH method was used to assess the distribution of the pore sizes, as summarized in Table 2. According to the IUPAC classification, the isotherms of SF/SS showed a type-II isotherm curve, indicating the presence of mesoporous material (>50 nm) [25]. The IUPAC-classified H3 type hysteresis loops are not within the typical BET range. Additionally, the sort of hysteresis loops seen in these isotherms suggests that they may have been caused by the shape of the pores. Compared to the SF/SS (3:2), the SF/SS (4:1) exhibited a larger specific surface area (i.e., 11.58 m<sup>2</sup>·g<sup>-1</sup> to 9.57 m<sup>2</sup>·g<sup>-1</sup>). The average pore size for SF/SS (3:2) and SF/SS (4:1) was found to be 12.47 nm and 19.32 nm, respectively, according to the BJH technique for determining the pore size distribution, showing the presence of mesopores. The pore structure exhibited a pore volume of 0.00571 and 0.00714 cc/g for the SF/SS (3:2) and the SF/SS (4:1), respectively. Further, the pore size distribution curve

indicates that both SF/SS compositions had a bimodal pore structure with two pore diameter peaks. The findings show that the interior structure of the SF/SS bio-composite contained microporous and mesoporous structures.



**Figure 3** BET adsorption-desorption isotherm of bio-composite adsorbent with SF/SS compositions (4:1) and (3:2), respectively. The inset shows the BJH pore size distribution.

**Table 2** Surface and pore characteristics at two SF/SS ratios.

SF/SS compositions	Average pore diameter (nm)	Specific surface area (m²/g)	Pore volume (cc/g)
3:2	12.47	9.57	0.00571
4:1	19.32	11.58	0.00714

### 3.2 Adsorption of CV and Ion Cu<sup>2+</sup> onto SF/SS Bio-composite

The CV adsorption performance for the utilization of different SF/SS compositions was observed after 120 min to attain its equilibrium condition (Figure 4(a)). In comparison to the other materials, it was discovered that ratio of 4:1 SF:SS exhibited the highest adsorption capability. This is plausible since according to SEM and BET characterization, the SF/SS (4:1) adsorbent possessed the highest surface area and pore volume compared to the other adsorbents, which allows for a higher adsorption capability. As a result, the remaining adsorption

test only covered the SF/SS (4:1) sample. Irrespective of the initial organic dye concentration, it was shown that the CV dye molecule was quickly adsorbed onto SF/SS (4:1) within 20 min, and the adsorption rate thereafter decreased prior to reaching equilibrium state in 120 min, as depicted in Figure 4(b). The noncompetitive adsorption process occurring on the active surface sites of the adsorbent may be the cause of the rapid adsorption in the first 20 minutes, while the lack of available adsorption sites as the monolayer adsorption on the surface approaches completion may be the cause of the slow process that follows. Overall, the findings demonstrate that the adsorption performance of SF/SS (4:1) toward the organic dye model is independent of the dye concentration in the solution.

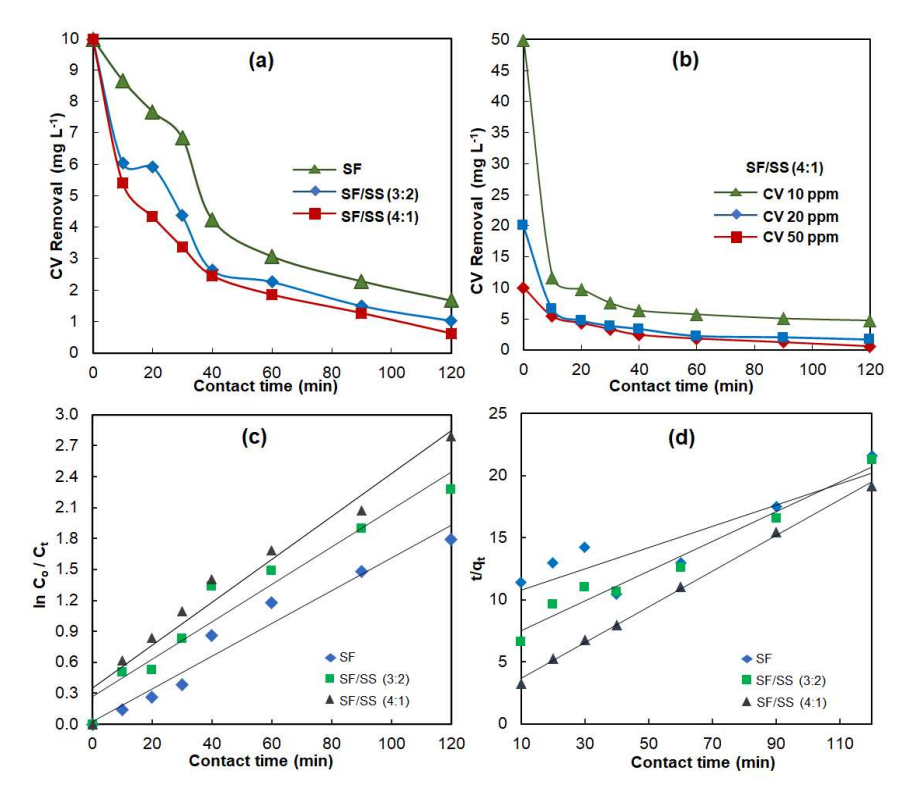


**Figure 4** (a) Crystal violet removal using pristine SF and SF/SS composites; (b) crystal violet removal (mg. L-1) through adsorption on SF/SS (4:1) composite under different initial dye concentration; (c) linear dependence of Ct/Co on the PSO model and (d) the PSO derived plot of t/Qt vs t.

To understand the underlying mechanism of organic dye and heavy metal ion adsorption, the adsorption kinetic of crystal violet onto both SF and SF/SS

adsorbent was modeled using pseudo-first (PFO) and pseudo-second order (PSO) models. The linear plot of  $\ln{(C_o/C_t)}$  vs t (Figures 4(c)) and  $t/q_t$  vs t (Figures 4(d)) represents the data fitting according to the PFO and the PSO model, respectively, which is mathematically expressed as follows:

PFO: 
$$ln(C_o - C_t) = lnC_o - k_1 t$$
 (1)

$$PSO: \frac{t}{q_t} = \left(\frac{1}{k_2 q_e^2}\right) + \frac{t}{q_e} \tag{2}$$

where  $C_o$  and  $C_t$  are the concentration of the crystal violet at the initial condition and at time t, respectively. The amount of crystal violet adsorbed at time t and at equilibrium state is represented by  $q_t$  and  $q_e$ , respectively. The adsorption rate  $k_1$  (min<sup>-1</sup>) and  $k_2$  (m·g<sup>-1</sup>·min<sup>-1</sup>) is determined using linear fitting analysis following the PFO and the PSO model, respectively [26,27]. The estimated adsorption capacity (calculated  $C_t$ ) for the PSO model best fit the experiment results as indicated by the higher  $R^2$  than that for PFO model (Table 3).

**Table 3** Rate constant of CV adsorption as the effect of SF/SS compositions derived from PFO and PSO models.

Sample	$k_1 \times 10^{-3}$ (min <sup>-1</sup> )	$\mathbb{R}^2$	$k_2 \times 10^{-3}$ (min <sup>-1</sup> )	R <sup>2</sup>
SF only	$k_{obs} = 15.82$	0.9605	$k_{obs}=8.67$	0.9652
SF/SS (3:2)	$k_{obs} = 18.11$	0.9404	$k_{obs} = 41.71$	0.9827
SF/SS (4:1)	$k_{obs} = 20.85$	0.9576	$k_{obs} = 63.39$	0.9977

The experimental data did not completely fit the linear fitting curve for Cu<sup>2+</sup> ion removal. This finding suggests that rate-controlling processes other than intraparticle diffusion also occurred. The significant intercept of the linear fit also suggests that the adsorption rate is controlled by mass transfer [28]. The adsorption of Cu<sup>2+</sup> ions on SF/SS was observed using an isothermal adsorption study to fully explain the adsorption behavior. It is possible to use adsorption isotherms to explain equilibrium data as well as adsorption properties. The best model fitting to the adsorption data at the equilibrium state must be found to understand the adsorption mechanism as well as possible. In this work, the adsorption process was examined using the *Langmuir* and *Freundlich* adsorption isotherms. The adsorption isotherm by *Langmuir* assumes that the Cu<sup>2+</sup> adsorption forms a monolayer on a homogeneous surface [29]. This *Langmuir* model is mostly employed to evaluate the adsorption mechanism at the adsorption equilibrium. The *Langmuir* model is expressed as follows:

$$\frac{c_e}{q_e} = \frac{1}{q_{max}k_L} + \frac{c_e}{q_{max}}\frac{c_e}{q_e} = \frac{1}{q_{max}k_L} + \frac{c_e}{q_{max}}$$
(3)

where  $q_e$  is the equilibrium amount of adsorbed  $Cu^{2+}$ ,  $q_{max}$  is the highest amount of composite SF/SS adsorbed, and  $k_L$  is the adsorption constant of *Langmuir*,  $C_e$  is the  $Cu^{2+}$  concentration at equilibrium state (mg·g<sup>-1</sup>). The *Freundlich* isotherm is modeled as follows:

$$ln(q_e) = k_F + \frac{1}{n}lnC_e \tag{4}$$

where  $k_F$  represents the isotherm constant, and 1/n indicates the mode of adsorption toward the adsorbent surface. Chemisorption is indicated by n < 1, while physisorption is indicated by n > 1 [30].

**Table 4** Adsorption parameters following the Langmuir and Freundlich isotherm models for CV and Cu2+ removal.

Isotherms	Parameters	CV Adsorption	Cu <sup>2+</sup> Adsorption
Langmuir	$q_m (mg \cdot g^{-1})$ $K_L (mg \cdot L^{-1})$	78.62 0.117	69.22 0.087
	$R^{2}$	0.89	0.97
	$K_F (mg \cdot g^{-1})$	8.376	5.732
Freundlich	1/n	0.771	0.773
	$\mathbb{R}^2$	0.97	0. 99

The linear fit parameter, i.e., slope and intercept, were utilized to determine q<sub>max</sub>, k<sub>L</sub>, and k<sub>F</sub>, which are summarized in Table 4. According to R<sup>2</sup>, Cu<sup>2+</sup> adsorption onto SF/SS follows Freundlich model. Additionally, R<sup>2</sup> for both the Freundlich and the Langmuir model, a was higher than 0.97, demonstrating that the composite SF/SS (4:1) adsorption process also fit well with the Langmuir adsorption isotherm. The fact that n > 1 was seen for the Freundlich model indicates that the adsorption mechanism of both CV and Cu<sup>2+</sup> onto SF/SS biocomposite is dominated by a physisorption process. Although physisorption dominates the adsorption process, the chemical interaction is apparent from the IR spectrum of post-adsorption sample. It is possible that the adsorption of Cu<sup>2+</sup> onto SF/SS modifies the β-sheet conformation and the electrostatic interaction between the cation and either the negative dipole of carboxylic acid or the positive dipole of amide functional groups affect the chemisorption process. Furthermore, the higher adsorption capacity for SF/SS (4:1) than for SF/SS (3:2) suggests that a higher SF fraction can enhance the adsorption capacity. The current results of SF/SS (4:1) for Cu<sup>2+</sup> removal in aqueous solutions is on par with the results in the literature, where the adsorption capacity was found to be 69.22 mg·g<sup>-1</sup> compared to SF-based adsorbent with 74.63 mg·g<sup>-1</sup> [25].

#### 4 Conclusion

In this work, a novel silk fibroin-based bio-composite adsorbent using a wetchemical method was developed. The soursop seed (SS) composition in the composites affected the morphological and adsorption performance, where the optimum composition was obtained for SF/SS (4:1). The as-prepared bio-composite SF/SS (4:1) was able to adsorb Cu<sup>2+</sup> and crystal violet (CV) dye up to 87.3 and 93.7%, respectively. The pseudo-second order best fit the kinetic data, yielding the kinetic rate constants of pristine SF ( $k_2 = 15.82 \times 10^{-3} \, \text{min}^{-1}$ ), SF/SS (3:2) with  $k_2 = 18.11 \times 10^{-3} \, \text{min}^{-1}$ ), and SF/SS (4:1) with  $k_2 = 20.85 \times 10^{-3} \, \text{min}^{-1}$ . The adsorption isotherm followed the Freundlich model with a maximum adsorption capacity or  $K_F$  of 8.37 mg·g<sup>-1</sup> and a value of 1/n of 0.771, which indicates that the adsorption mechanism of CV dye on the SF/SS composite was physisorption. Similarly, the physisorption of ion Cu<sup>2+</sup> on the SF/SS composite resulted in a adsorption capacity of 5.73 mg·g<sup>-1</sup>. Based on the findings of this study, SF/SS may be used as a bio-sorbent to effectively remove heavy metals and organic dyes from wastewater.

The present result highlights the practical application of our novel and sustainable bio-based adsorbent material. For further study, we suggest optimizing the composition of the SF/SS bio-composite adsorbent with finer increments of SS mass fraction in the composite as the phytic acid based cross linking agent may show a controlling pattern toward the defined microstructure. In addition, comprehensive investigation should exploit other possible natural cross-linking agents extracted from soursop seeds and a detailed investigation on the underlying pore opening/closing on SF-based adsorbent should be carried out.

#### Acknowledgments

The Kurita Water Environment Foundation (KWEF) grant with award number 19Pid021 is acknowledged by the authors as the source of their financial support. We gladly recognize the technical assistance provided by the National Research and Innovation Agency (BRIN), the central laboratory of mineral and advanced material at Universitas Negeri Malang (UNM), and Universitas Negeri Semarang (UNNES) for sample characterization.

#### References

- [1] Indonesia Industrial Estates Directory, *Kariangau Industrial Area*, 2019. (Text in Indonesian)
- [2] Summary Environmental Impact Assessment, *Inter-Island Transport Project (Ports) in Indonesia*, 2005.

- [3] Saibun Sitorus, S., Yerwanto, I. & Nugroho, R.A., *Analysis of Metal Content of Pb, Cd, Cu, as in Water, Sediment and Bivalves, Balikpapan Bay Coast.*, Indonesian Environmental Dynamics, 7(2), pp. 89-94, 2020.
- [4] Tchounwou, P.B., Yedjou, C.G. & Sutton, D.J., *Heavy Metal Toxicity and the Environment*, Molecular-Clinical and Environmental Toxicology, Part of the Experientia Supplementum Book Series, **101**, pp. 133-164, 2012.
- [5] Jeirani, Z., Niu, C.H. & Soltan, Adsorption of Emerging Pollutants on Activated Carbon, J. Rev. Chem. Eng., 33(5), pp. 491-522, 2017.
- [6] Ani, J.U., Akpomie, K.G., Okoro, U.C., Aneke, L.E., Onukwuli, O.D. & Ujam, O.T., Potentials of Activated Carbon Produced from Biomass Materials for Sequestration of Dyes, Heavy Metals, and Crude Oil Components from Aqueous Environment, Appl. Water Sci., 10(69), pp. 1-11, 2020.
- [7] Yuen, F.K. & Hameed, B.H., Recent Developments in The Preparation and Regeneration of Activated Carbons by Microwaves, Adv. Colloid Interface Sci., 149(1), pp.19-27, 2009.
- [8] Sharma, P. K, Ayub, S. & Tripathi, C. N., Agro and Horticultural Wastes as Low-Cost Adsorbents for Removal of Heavy Metals from Wastewater: A Review, International Refereed Journal of Engineering and Science (IRJES), 2(8), pp. 18-27. 2013.
- [9] Deniz, F. & Ersanli, E.T., A Renewable Biosorbent Material for Green Decontamination of Heavy Metal Pollution from Aquatic Medium: A Case Study on Manganese Removal, Intern. J. Phytoremediation, 23(3), pp. 231-237, 2021.
- [10] Chuah, T.G., Jumasiah, A., Azni, I., Katayon, S. & Thomas Choong, S.Y., *Rice Husk as A Potentially Low-Cost Biosorbent for Heavy Metal and Dye Removal: An Overview*, Desalination, **175**(3), pp. 305-316, 2005.
- [11] Crini, G., Lichtfouse, E., Wilson, L.D. & Morin-Crini, N., *Conventional and Non-Conventional Adsorbents for Wastewater Treatment*, Environ. Chem. Lett., 17, pp. 195-213, 2019.
- [12] De Gisi, S., Lofrano, G., Grassi, M. & Notarnicola, M., Characteristics and Adsorption Capacities of Low-cost Sorbents for Wastewater Treatment: A Review. Sustain. Mater. Technologies, 9, pp. 10-40. 2016.
- [13] Cao, Y. & Wang, B., *Biodegradation of Silk Biomaterials*, Int. J. Mol. Sci., **10**, pp. 1514-1524, 2009.
- [14] Hu, X., Shmelev, K., Sun, L., Gil, Eun-Seok, Park, S.H., Cebe, P. & Kaplan, D.L., *Regulation of Silk Material Structure by Temperature-Controlled Water Vapor Annealing*, ACS. Biomacromolecules, **12**(5), pp. 1686-1696, 2011.
- [15] Kim, U.J., Park, J., Li, C., Jin, H.J., Valluzzi, R. & Kaplan, D.L., *Structure and Properties of Silk Hydrogels*, ACS. Biomacromolecules, **5**(3), pp. 786-792, 2004.

- [16] Kundu, S.C., Dash, B.C., Dash, R. & Kaplan, D.L., *Natural Protective Glue Protein, Sericin Bioengineered by Silkworms: Potential for Biomedical and Biotechnological Applications*, Progress in Polymer Science., **33**(10), pp. 998-1012, 2008.
- [17] Campagnolo, L., Morselli, D., Magri, D., Scarpellini, A., Demirci, C., Colombo, M., Athanassiou, A. & Fragouli, D., Silk Fibroin/Orange Peel Foam: An Efficient Biocomposite for Water Remediation, Adv. Sustain. Syst., 3(1), 1800097, 2019.
- [18] Sato, T., Seki, T., Yokoyama, S. & Ito, S., Adsorption of Cesium Ion on Silk Fibroin in Aqueous Solution, Trans. Mater. Res. Soc. Jpn., 42(2), pp. 19–22. 2017.
- [19] Ernawati, L., Wahyuono, R.A., Halim, A., Noorain, R., Widiyastuti, W., Dewi, R.T. & Enomae, T., *Hierarchically 3-D Porous Structure of Silk Fibroin-Based Biocomposite Adsorbent for Water Pollutant Removal*, Environments, **8**(11), 127, 2021.
- [20] Ocampo-Pérez, R., Leyva-Ramos, R., Sanchez-Polo, M. & Rivera-Utrilla, J., Role of Pore Volume and Surface Diffusion in the Adsorption of Aromatic Compounds on Activated Carbon, J. Adsorption, 19, pp. 945-957. 2013.
- [21] Kamalha, E., Zheng, Y.S., Zeng, Y.C., Fredrick, M.N., FTIR & WAXD Study of Regenerated Silk Fibroin, Adv. Mater. Res., 677, pp. 211-215, 2013.
- [22] Ki, C.S., Park, Y.H. & Jin, H.J., Silk Protein as A Fascinating Biomedical Polymer: Structural Fundamentals and Applications, Macromol. Res., 17, pp. 935-942, 2009.
- [23] Asakura, T., Yao, J., Yamane, T., Umemura, K. & Ulrich, A.S., *Heterogeneous Structure of Silk Fibers from Bombyx mori Resolved by 13C Solid-State NMR Spectroscopy*, J. Am. Chem. Soc., **124**(30), pp. 8794–8795. 2002.
- [24] Zhang, M., Yin, Q., Ji, X. Wang, F., Gao, X. & Zhao, M, High and Fast Adsorption of Cd(II) And Pb(II) Ions from Aqueous Solutions by a Waste Biomass Based Hydrogel. Sci Rep., 10, 3285, 2020.
- [25] Rastogi, S. & Kandasubramanian, B., *Progressive Trends in Heavy Metal Ions and Dyes Adsorption Using Silk Fibroin Composites*, Environ Sci Pollut Res., **27**, pp. 210-237, 2020.
- [26] Hameed, B.H., Mahmoud, D.K. & Ahmad, A.L., Equilibrium Modeling and Kinetic Studies on the Adsorption of Basic Dye by a Low-Cost Adsorbent: Coconut (Cocos Nucifera) Bunch Waste, J. Hazard. Mater, 158(1), pp. 65-72, 2008.
- [27] Wang, S., Ning, H., Hu, N., Huang, K., Weng, S., Wu, X., Wu, L. & Liu, J., Alamusi, Preparation and Characterization of Graphene Oxide/Silk Fibroin Hybrid Aerogel for Dye and Heavy Metal Adsorption, Compos. Part B Eng., 163, pp. 716-722. 2019.

- [28] Rudzinski, W. & Plazinski, W., Kinetics of Solute Adsorption at Solid/Solution Interfaces: A Theoretical Development of the Empirical Pseudo-First and Pseudo-Second Order Kinetic Rate Equations, based on Applying the Statistical Rate Theory of Interfacial Transport, ACS. J. Phys. Chem. B., 110(33), pp. 16514-16525, 2006.
- [29] Khayyun, T.S. & Mseer, A.H., Comparison of The Experimental Results with the Langmuir and Freundlich Models for Copper Removal on Limestone Adsorbent, Appl. Water Sci., 9, pp. 170, 2019.
- [30] Chung, H.K., Kim, W.H., Park, J., Cho, J., Jeong, T.Y. & Park, P.K, Application of Langmuir and Freundlich Isotherms to Predict Adsorbate Removal Efficiency or Required Amount of Adsorbent, J. Ind. Eng. Chem, 28(6), pp. 241-246, 2015.